Monitoring and Analyzing Uplift Pressure within the Dam Foundation of Wanmipo Hydropower Station

Wenfeng Ma [1], Zhaoyang Li [1], Hui Shen [1], Qi Ling [1], and Xiaolong Lv [2*]

[1]Nanjing NARI Water Resources and Hydropower Technology Company Limited, Nanjing, Jiangsu, China
[2]College of Mechanics and Materials, Hohai University, Nanjing, Jiangsu, China

*Corresponding author's e-mail: lyuxl@hhu.edu.cn

Abstract. Uplift pressure within the dam foundation is crucial for maintaining the stability of gravity dams and serves as a pivotal metric in evaluating dam safety. This study evaluates the uplift pressure characteristics of the Wanmipo Hydropower Station's dam, drawing upon years of accumulated monitoring data. Using process curve analysis, spatial distribution, and statistical modeling, we conducted an in-depth analysis of the uplift pressure data from both qualitative and quantitative perspectives. We also evaluated the efficacy of the dam's grout curtain in decreasing seepage. Our findings reveal that the temporal and spatial variations of uplift pressure are within expected norms, the grout curtain effectively mitigates upstream water levels, and seepage within the dam foundation has reduced after years of operation.

Keywords: Dam safety; concrete gravity dam; uplift pressure of dam foundation; statistical model; monitoring data

1 Introduction

Dams play a crucial role in supporting local economies and protecting lives and assets. Thus, consistent monitoring of these structures is indispensable. By employing a range of monitoring devices at specific sites within the dam and subsequently having experts assess the data, we can obtain a comprehensive view of the dam's safety status.

The response monitoring of dam deformation, seepage, and other reactions to the structural state of the dam is influenced by various factors such as environmental quantity and its own structure, and the mechanism relationship between response monitoring and influencing factors is difficult to accurately obtain. Therefore, in practical engineering, monitoring data is often analyzed through some mathematical models. As early as 1955, Feneli from the Institute of Structure and Modeling (ISMES) of the Italian State Electricity Authority and Rocha et al. from Portugal [1] applied statistical regression methods to quantitatively analyze deformation observation data of dams. In 1965, Tonini from Italy [2] first classified the factors that affect dam displacement into the forms of water pressure, temperature, and aging components. Subsequently, the statis-

D. Li et al. (eds.), *Proceedings of the 2023 9th International Conference on Architectural, Civil and Hydraulic Engineering (ICACHE 2023)*, Advances in Engineering Research 228,
https://doi.org/10.2991/978-94-6463-336-8_68

tical modeling method based on the combination of effect quantity separation and regression became one of the mainstream methods for analyzing dam monitoring data [3-5].

In addition, the use of finite element models for deterministic analysis of dam deformation, seepage, etc. is also widely used. Wu Zhongru, Liu Guanbiao, et al. [6] applied a deterministic model to the analysis of horizontal displacement at the top of the Fozi-ling multi-arch dam. The calculated values using the finite element method were fitted with the measured values using the least squares method to obtain the adjustment parameters and time effect components of the water pressure and temperature components, proving that the model has high fitting accuracy and reliable posterior prediction. Li Danjiang et al. [7] applied a hybrid model combining finite element and statistical analysis to the analysis of observation data of Hengshan Arch Dam, believing that this model has the characteristics of less mechanical calculation, wide applicability, and high reliability, while taking into account the advantages of both statistical and mechanical analysis models. However, due to the time-consuming establishment of finite element models for dams and the need for extensive calibration and verification of model accuracy, this method is usually not the preferred method for monitoring data analysis in dam operation management.

A critical metric in this assessment is the uplift pressure within the dam's foundation. This pressure is essential in determining the stability of gravity dams. By analyzing its distribution across time and space, we can discern patterns, detect anomalies, and thereby enhance our understanding of the dam's resistance to sliding. This knowledge also informed us about the effectiveness of measures such as the grout curtain in decreasing seepage. In this study, we integrated qualitative techniques, like spatial and temporal pattern assessments, with quantitative statistical analyses. Using data sourced from the Wanmipo Hydropower Station, we carried out a detailed examination of the uplift pressure's distribution while also evaluating the efficacy of the grout curtain.

2 Project Overview

The dam at Wanmipo Hydropower Station is a roller-compacted concrete gravity dam with a height of 66.5 m and a crest length of 238 m, segmented into ten sections. The reservoir operates at a standard water level of 248 m and has a minimum usable level of 238 m, providing a total capacity of 378 million m³. Since its commissioning in 2004, the dam consistently performed well, achieving Level A in its inspections of October 2010 and November 2015. Notably, from 2015 to 2020, discrepancies in some uplift pressure readings were observed. Given the importance of uplift pressures for dam stability [1, 5, 8–10], a rigorous analysis of their distribution and trends is crucial.

To meticulously monitor the uplift pressure of the dam's foundation, 12 monitoring holes were positioned within the foundation gallery. Each hole was equipped with automated pressure measurement tubes, as detailed in Fig. 1. In 2015, an enhancement of the monitoring setup led to the addition of two more observation holes adjacent to the original BO12 measuring hole, spaced 1 meter downstream. These new additions were designated as BO12-1 and BO12-2. Notably, these new holes did not have automated

sensors, and thus, manual readings on site were required. To counteract potential disturbances from mountain water infiltration at the BO12 measurement location, three drainage outlets were strategically positioned about 1 meter high on the right wall of BO12, uniformly placed from the upstream to the downstream direction. Piezometers were also placed at specific cross-sectional locations in dam sections 3#, 5#, and 8# for more comprehensive surveillance. As a representation, the piezometer arrangement in dam section 8# is portrayed in Fig. 2.

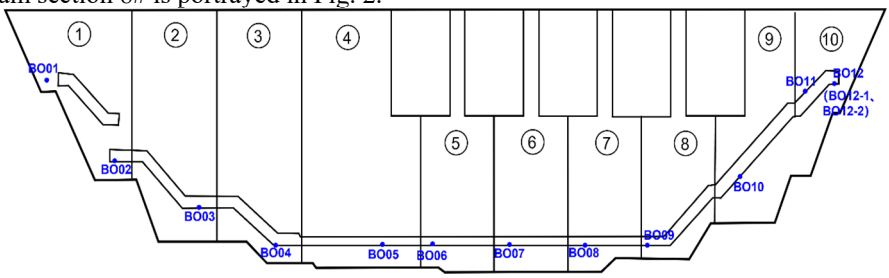

Fig. 1. Layout of uplift pressure measuring holes for dam foundation gallery

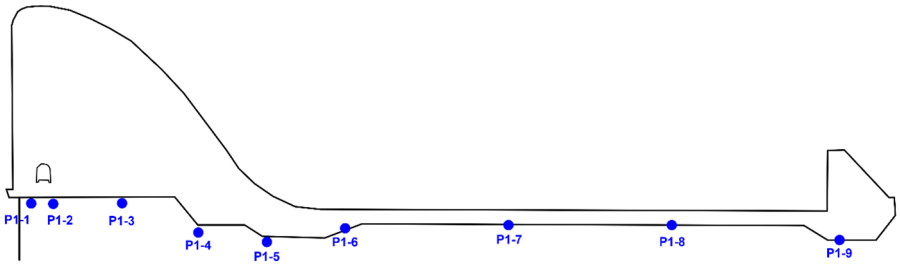

Fig. 2. Layout of osmometer at monitoring section of dam section 8#

3 Analysis of Monitored Values

3.1 Analysis of Process Curve

The examination of uplift pressure within dam foundations has been discerned through the meticulous crafting of a process curve, correlating multi-year water head height with upstream water levels within the base grouting gallery's uplift hole. The longitudinal assessment along the dam reveals noteworthy stability in uplift water levels across the majority of the dam foundation's measuring holes, thereby illustrating the dam foundation curtain's substantial anti-seepage efficacy. Instrument readings from locations BO02 and BO11 uncover subtle annual variations attributable to temperature fluctuations, suggesting the benign presence of diminutive fractures beneath the measuring holes. In contrast, data from BO03 exhibit conformance to upstream water level fluctuations, albeit with a numerical deviation of approximately 30 meters, indicating a predominant influence of water pressure, which is effectively mitigated by the anti-

seepage curtain. BO09's readings elucidate a gradual increment, attributable to perpetually generated gas within the measuring hole, with a stabilization of pressure values following the implementation of an exhaust pipe to vent extraneous gas. Notably, BO12 readings manifest prominent annual fluctuations concomitant with upstream water levels, maintaining relative proximity thereto. Conversely, BO12-1 and BO12-2, situated downstream on BO12's identical monitoring section, present conspicuously lower water heads and exhibit attenuated variations with upstream levels. This fosters a preliminary hypothesis positing BO12's location ahead of the curtain, thereby rendering its data non-reflective of the curtain's anti-seepage proficiency.

Most seepage pressure meters, distributed across three monitoring cross-sections, predominantly negated the detection of water pressure, and those few that were impacted primarily echoed influences from downstream water levels, thereby further substantiating the dam foundation curtain's potent anti-seepage efficacy.

3.2 Analysis of Spatial Distribution Patterns

(1) Uplift Pressure Analysis in Longitudinal Section

An analysis was conducted on the longitudinal section, hosting 12 pressure gauges within the dam foundation's grouting gallery. Two particular instances were evaluated, namely, February 25, 2020 (with an upstream water level of 239.15 m and downstream of 202.62 m), and July 15, 2020 (upstream at 246.93 m, downstream at 204.55 m). Figure 3 illustrates the distribution diagram, providing insights into the longitudinal uplift water level across the dam base. The distribution generally mirrors a pattern wherein the uplift water levels at the left and right bank gravity dam sections are elevated, juxtaposed with notably lower levels at the central section, with the plant dam section revealing the lowest. This distribution aligns significantly with the extensive fluctuations observed in the dam bottom elevation [11]. Aside from the measuring holes BO09 and BO12, uplift water level variations at other holes remain nominal during spring and summer, substantiating the commendable anti-seepage efficacy of the dam foundation curtain.

(2) Transverse Uplift Pressure Analysis

Accounting for the integrity of existing monitoring devices, the transverse monitoring section of the #8 spillway dam segment is selected for analyzing the transverse distribution of foundation uplift pressure. A characteristic measurement was taken on July 25, 2020 (upstream water level: 246.46 m), with the transverse distribution of the foundational uplift pressure (see Fig. 4). Figure 4 illustrates that the foundation curtain significantly impedes the permeation from upstream high water pressure, presenting a smooth transition in uplift water head changes across measuring holes behind the curtain, and collectively exhibiting a linear configuration.

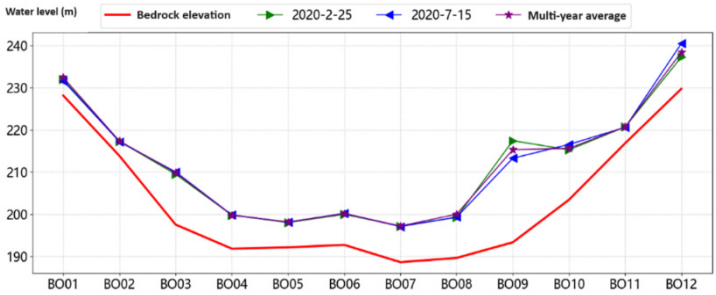

Fig. 3. Longitudinal distribution diagram of uplift pressure of dam foundation

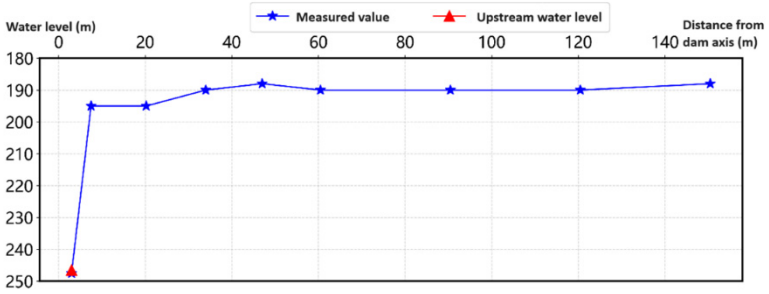

Fig. 4. Transverse distribution diagram of uplift pressure at dam foundation of the dam section 8#

4 Analysis of Factors Influencing Uplift Pressure

4.1 Selection of Key Factors

Based on insights from prior studies [12–14], the primary variables influencing uplift pressure include downstream and upstream water pressure, temperature, rainfall, and time effects. As the dam's downstream water level exhibits limited variability and consistently remains at a lower range, the effect of downstream water pressure has been omitted. The statistical model for recording uplift pressure observations is delineated below.

$$H = H_{hu} + H_T + H_P + H_\theta \tag{1}$$

where H_{hu} represents the upstream water pressure component; H_T represents the temperature component; H_P represents the rainfall component; and H_θ represents the time effect component.

(1) Water Pressure Component

The water pressure component is derived from a polynomial of water levels and their recent average, as expressed below.

$$H_{hu} = \sum_{i=1}^{3} a_i h^i + a_4 h_0 + a_5 \bar{h}_{1\sim3} + a_6 \bar{h}_{4\sim15} + a_7 \bar{h}_{16\sim30} \tag{2}$$

Where h^i ($i = 1, 2, 3$) is the exponential term related to the water level; h_0 is the reservoir water level on the observation day; $\bar{h}_{1\sim3}$ is the average reservoir water level over the prior 1 to 3 days, and similarly, $\bar{h}_{4\sim15}$ and $\bar{h}_{16\sim30}$ refer to the average water levels from the preceding 4 to 15 days and 16 to 30 days, respectively; a_i ($i = 1, 2, \ldots, 7$) is the regression coefficient corresponding to each factor of the water pressure component.

(2) Temperature Component

The temperature of the dam foundation is predominantly governed by the influence of ambient and groundwater temperatures. Direct measurement of its precise value is unattainable; hence, an approximation is achieved using ambient temperature values. A time-dependent trigonometric function is introduced to depict the periodicity of temperature variations. The expression is delineated below:

$$H_T = b_1 T_0 + b_2 \bar{T}_{1\sim3} + b_3 \bar{T}_{4\sim15} + b_4 \bar{T}_{16\sim30} + \sum_{j=1}^{2} \left[b_{1j} \sin \frac{2\pi jt}{365} + b_{2j} \cos \frac{2\pi jt}{365} \right] \quad (3)$$

where T_0 is the temperature on the observation day; $\bar{T}_{1\sim3}$ is the average temperature over the preceding 1 to 3 days, similarly for $\bar{T}_{4\sim15}$ and $\bar{T}_{16\sim30}$; t is the cumulative days since the beginning of observation; b_i ($i = 1, 2, \ldots, 4$), b_{1j}, and b_{2j} ($j = 1, 2$) are the regression coefficients of each factor within the temperature component.

(3) Rainfall Component

The expression for the rainfall component is as follows:

$$H_P = \sum_{i=1}^{4} c_i \bar{P}_i \quad (4)$$

where $\bar{P}_i$ ($i = 1, 2, \ldots, 4$) denotes the average rainfall values for distinct periods: the observation day, preceding 1 to 3 days, 4 to 14 days, and 16 to 30 days, organized according to the subscript i; c_i is the regression coefficient corresponding to each impacting factor of the rainfall component.

(4) Time Effect Component

The intricacy of the mechanisms whereby temporal effects modulate uplift pressure at the dam foundation is pronounced. Aligning with established research, this can be delineated as a linear combination of first-order and logarithmic terms related to time:

$$H_\theta = d_1 \theta + d_2 ln\theta \quad (5)$$

where $\theta = t/100$; d_1 and d_2 denote the regression coefficients corresponding to each factor within the time effect component.

4.2 Analysis of Influencing Factors

Employing statistical model (1), stepwise regression analysis is conducted on the observational data from 2015 to 2020 pertaining to the uplift water levels of the dam foundation in the gallery (BO01–BO12). Correlation coefficients and residual standard deviations, correlated with each observational hole within the statistical models, are detailed in Table 1. It reveals that the overall integrity of the uplift water level statistical models for the dam foundation is not robust. Among the 12 statistical models, only the

BO03 measuring hole has a complex correlation coefficient reaching 0.90, while others, such as BO07, BO08, BO10, and BO11 exceed 0.80, reflecting the systematic nature of the measured uplift water levels. The complex correlation coefficients for the remaining holes do not surpass 0.8, with particular holes like BO01 and BO05 falling below 0.50, thereby failing to reliably mirror the variability of uplift water levels with assorted influencing factors. Considering the onsite inspection circumstances and monitoring system maintenance status, the inferior quality of some measurement hole's statistical models primarily originates from various interference factors, such as disturbances to instruments during manual maintenance and abnormal instances (such as BO09's air pressure).

Table 1. Statistical Model of BO01–BO12 Uplift Pressure Water Level

Measuring Holes	Coefficient of Multiple Correlation R	Residual Standard Deviation S (Unit: m)
BO01	0.19	0.253
BO02	0.62	0.093
BO03	0.90	0.143
BO04	0.56	0.219
BO05	0.37	0.186
BO06	0.78	0.283
BO07	0.81	0.106
BO08	0.80	0.341
BO09	0.47	3.697
BO10	0.87	0.352
BO11	0.83	0.121
BO12	0.71	1.316

An enhanced analysis was performed on the statistical models of measuring holes, specifically those with a complex correlation coefficient surpassing 0.80, with results outlined in Table 2. Our conclusions are detailed as follows:

1) Each of the five statistical models embeds water pressure and temperature components, affirming that the uplift pressure within the dam foundation is fundamentally governed by upstream water levels and temperature. Additionally, divergent models exhibit varied proportional relationships between water pressure and temperature components, illuminating the existence of permeability variances within the dam foundation across discrete dam sections.

Table 2. Proportion of each component of the statistical model for uplift water level of dam foundation(%)

Measuring Holes	Water Pressure	Temperature	Rainfall	Time Effects
BO03	73	15	12	0
BO07	28	72	0	0
BO08	11	89	0	0
BO10	24	58	0	18
BO11	17	83	0	0

2) Excluding BO03, the temperature components supersede water pressure components in the remaining models among the quintet of statistical models. According to extant research [13], variations in temperature may elicit alterations in the uplift water levels of the dam foundation by instigating expansion or occlusion of permeation channels—a scenario typically inescapable for roller-compacted concrete dams. A predominance of temperature components over water pressure components suggests the efficacy of the dam curtain in attenuating upstream water pressure, consequently lowering the aggregate impact of water pressure.

3) Only BO03 includes a rainfall component, constituting a mere 12%, suggesting a feeble correlation between the uplift pressure in the dam foundation and rainfall levels.

4) Only BO10 includes a temporal effect component, comprising a modest 18%. This suggests that subsequent to extended years of dam operation, fluctuations in the uplift pressure have largely stabilized, with no apparent variations [15].

5 Conclusions

Based on an exhaustive analysis of the uplift pressure data from Wanmipo Hydropower Station collected over several years, the following conclusions can be drawn.

The vertical distribution of uplift pressure in the dam foundation aligns consistently with the foundational topography, characterized by higher pressures on both sides and lower pressures in the central section. Horizontally, variations from the upstream to downstream are minimal, suggesting that the grout curtain effectively reduces the impact of the hydraulic head from the upstream area.

Statistical modeling reveals that the uplift pressure within the dam foundation is primarily modulated by temperature and upstream water levels, with negligible perturbations from rainfall or time effects. Following extended operational phases, dam foundation seepage has been controlled, absent of any discernible escalations or declinations in uplift pressure.

In summary, observed uplift pressures within the dam foundation conform to expected parameters, and the grout curtain has proven to be highly effective in preventing seepage.

References

1. Wu Z. R. Safety Monitoring Theory and Application in Hydraulic Structures. Nanjing: Hohai University Press; 2003.
2. Tonini D. Observed Behavior of Several Italian Arch Dams[J]. Journal of the Power Division, 1956, 82(6).
3. De Sortis A, Paoliani P. Statistical analysis and structural identification in concrete dam monitoring[J]. Engineering Structures, 2007, 29(1): 110-120.
4. Hu J, Ma F. Comprehensive Investigation Method for Sudden Increases of Uplift Pressures beneath Gravity Dams: Case Study[J]. Journal of Performance of Constructed Facilities, 2016, 30(5): 04016023.
5. Li X., Shang C. Analysis on monitoring results of foundation uplift pressure of a RCC gravity[J]. Yangtze River, 2015, 46 (21): 98-101.

6. Wu Z. R., Liu G. B. Research on the Deterministic Model of Displacement for Concrete Dams[J]. Dam Observation and Geotechnical Tests, 1987 (1): 16-25.
7. Li D.J., Yang L.X., Gu N. Hybrid model and its application in the analysis of original observation data of Hengshan arch dam[J]. Water Power, 1988 (5): 46-51.
8. Xiao X. L., Wan L., Shi Y. Q. Analysis of Abnormal Uplift Pressures under the Powerhouse Section in Fancuo Hydropower Station. Hydropower and New Energy.2016; (09): 1–4+12.
9. Zhu K., Mei Y. T., Liu J. Y., et al. Causal Analysis on Abnormity of Uplift Pressure of a Dam.Yangtze River. 2013; 44(01): 52–56.
10. Zhang F. Q., Wang Q. Analysis on Excessive Uplift Pressure of PushiheLower Reservoir Dam. Dam & Safety. 2020; (01): 42–44.
11. Tan L., Yang Y. Analysis of the Uplift Pressure Monitoring Data on Dam Foundation of Dongping Hydropower Station. Hydropower and New Energy. 2022; 36(02):59–64.
12. Zhang W. K., Xu M. H., Wang Y. T. Analysis of Uplift Pressure in the Lower Reservoir Dam Foundation of Guangzhou Pumped Storage Power Station. Water Resources and Power. 2014; 32(03): 115–117+24.
13. Liu S. D. Analysis of Uplift Pressure Observation Data for Guanyinyan Dam.Gansu Water Resources and Hydropower Technology. 2018; 54(09): 62–65.
14. Fan D. J., Ao S. F., Zhang Z. L. Analysis of Monitoring Data of the Foundation Uplift Pressure in Chaoyangsi Dam. Hydropower and New Energy. 2018; 32(07): 67–71.
15. Yang Q. Z. Analysis of Uplift Pressure Monitoring Data for a Gravity Dam. Science & Technology Vision. 2016;(26):358+372.